Co-activation of macrophages and T cells contribute to chronic GVHD in human IL-6 transgenic humanised mouse model

Rintaro Ono [a], Takashi Watanabe [b], Eiryo Kawakami [c], Makoto Iwasaki [a], Mariko Tomizawa-Murasawa [a], Masashi Matsuda [d], Yuho Najima [a], Shinsuke Takagi [e], Saera Fujiki [a], Rumi Sato [d], Yoshiki Mochizuki [b], Hisahiro Yoshida [d], Kaoru Sato [f], Hiromasa Yabe [f], Shunichi Kato [f], Yoriko Saito [a], Shuichi Taniguchi [e], Leonard D. Shultz [g], Osamu Ohara [b,h], Masayuki Amagai [i,j], Haruhiko Koseki [d], Fumihiko Ishikawa [a,*]

[a] Laboratory for Human Disease Models, RIKEN Center for Integrative Medical Sciences, Yokohama 230-0045, Japan
[b] Laboratory for Integrative Genomics, RIKEN Center for Integrative Medical Sciences, Yokohama 230-0045, Japan
[c] Disease Biology Group, RIKEN Medical Sciences Innovation Hub Program (MIH), Yokohama 230-0045, Japan
[d] Laboratory for Developmental Genetics, RIKEN Center for Integrative Medical Sciences, Yokohama 230-0045, Japan
[e] Department of Haematology, Toranomon Hospital, Tokyo 105-8470, Japan
[f] Department of Cell Transplantation and Regenerative Medicine, Tokai University School of Medicine, Isehara 259-1193, Japan
[g] The Jackson Laboratory, Bar Harbor 04609, ME, United States
[h] Department of Human Genome Research, Kazusa DNA Research Institute, Kisarazu 292-0818, Japan
[i] Laboratory for Skin Homeostasis, RIKEN Center for Integrative Medical Sciences, Yokohama 230-0045, Japan
[j] Department of Dermatology, Keio University School of Medicine, Tokyo 160-8582, Japan

ARTICLE INFO

ABSTRACT

Background: Graft-versus host disease (GVHD) is a complication of stem cell transplantation associated with significant morbidity and mortality. Non-specific immune-suppression, the mainstay of treatment, may result in immune-surveillance dysfunction and disease recurrence.

Methods: We created humanised mice model for chronic GVHD (cGVHD) by injecting cord blood (CB)-derived human CD34$^+$CD38$^-$CD45RA$^-$ haematopoietic stem/progenitor cells (HSPCs) into hIL-6 transgenic NOD/SCID/Il2rgKO (NSG) newborns, and compared GVHD progression with NSG newborns receiving CB CD34$^-$ cells mimicking acute GVHD. We characterised human immune cell subsets, target organ infiltration, T-cell repertoire (TCR) and transcriptome in the humanised mice.

Findings: In cGVHD humanised mice, we found activation of T cells in the spleen, lung, liver, and skin, activation of macrophages in lung and liver, and loss of appendages in skin, obstruction of bronchioles in lung and portal fibrosis in liver recapitulating cGVHD. Acute GVHD humanised mice showed activation of T cells with skewed TCR repertoire without significant macrophage activation.

Interpretation: Using humanised mouse models, we demonstrated distinct immune mechanisms contributing acute and chronic GVHD. In cGVHD model, co-activation of human HSPC-derived macrophages and T cells educated in the recipient thymus contributed to delayed onset, multi-organ disease. In acute GVHD model, mature human T cells contained in the graft resulted in rapid disease progression. These humanised mouse models may facilitate future development of new molecular medicine targeting GVHD.

Research in context

Evidence before this study

GVHD is an important complication of haematopoietic stem cell transplantation. Mouse models and clinical experience suggested important roles of activated T cells both in acute and chronic GVHD.

GWAS studies implicated IL-6 in pathogenesis of chronic GVHD and anti-IL6R Ab has been reported to ameliorate disease status in patients with chronic GVHD.

Added value of this study

We created a chronic GVHD humanised mouse model by transplanting human HSPCs into hIL-6 TG NSG newborns. In this model, activation of both human T cells and macrophages was associated with tissue damage in skin, lung, and liver. We also created acute

* Corresponding author at: 1-7-22 Suehiro-cho, Tsurumi-ku, Yokohama, Kanagawa 230-0045, Japan.
E-mail address: fumihiko.ishikawa@riken.jp (F. Ishikawa).
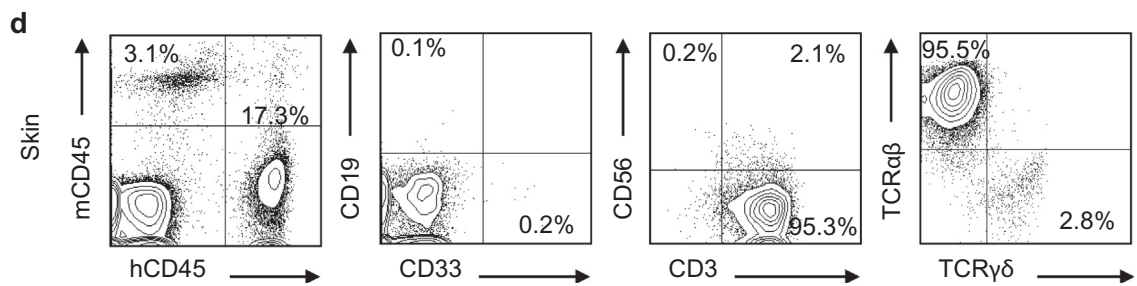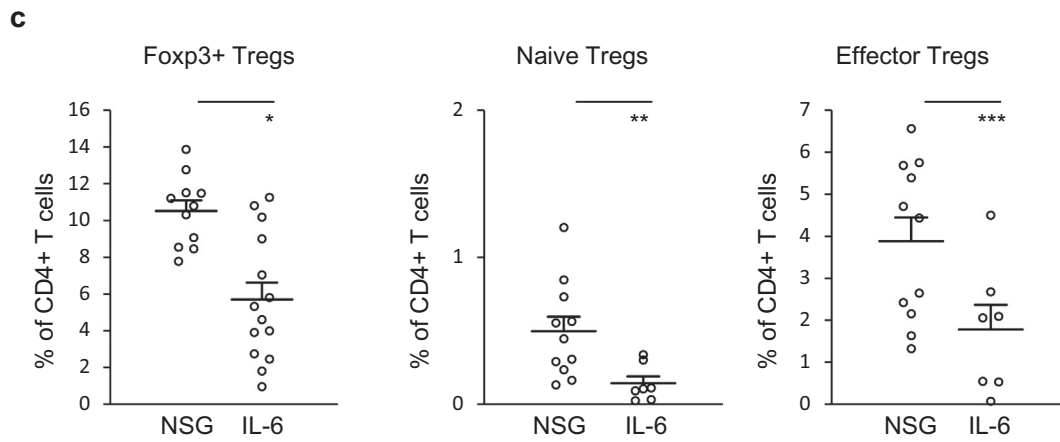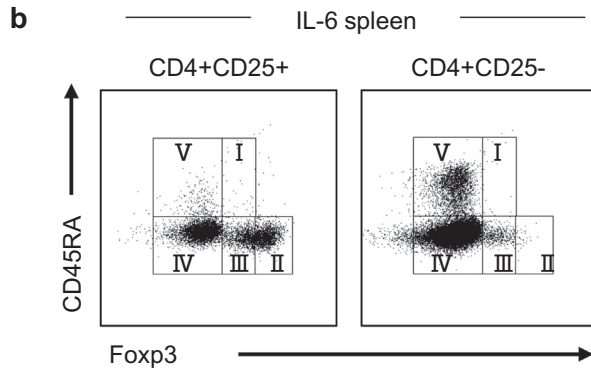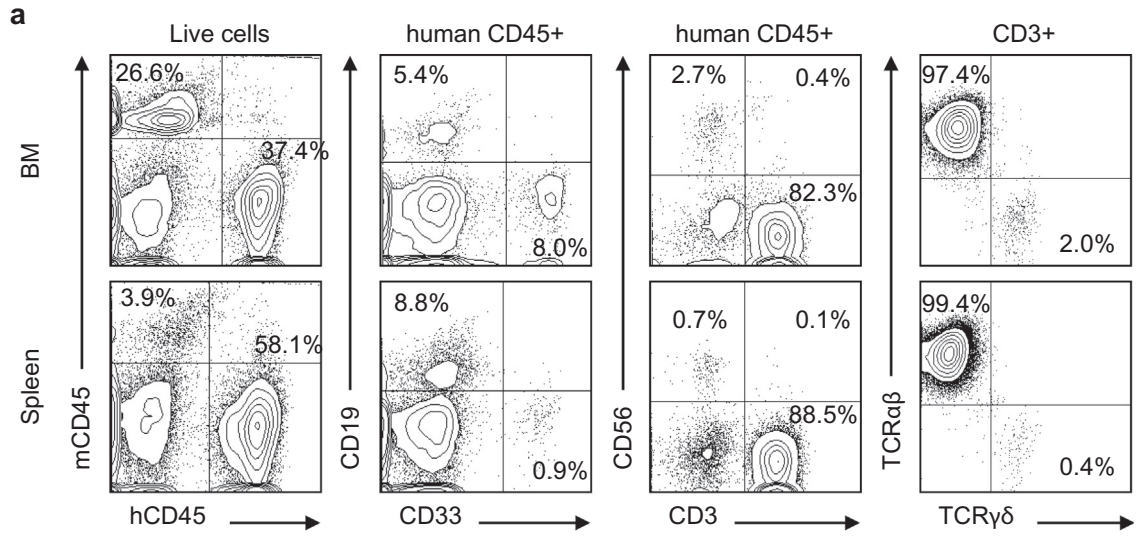
GVHD humanised mice by transplanting mature human leukocyte and myeloid cells to determine cellular and molecular distinction between acute and chronic GVHD. Through the comparison, we found that co-activation of fibrotic/sclerotic changes associated with T lymphocytes and macrophages in affected organs and higher expression of genes associated with TGF-β and SMAD signaling are characteristic of chronic GVHD.

Implications of all the available evidence

Our study revealed an important role of IL-6 and subsequent macrophage/T cell co-activation in the development of chronic GVHD. The preclinical humanised mouse model may serve as a beneficial tool for the investigation of chronic GVHD biology and new treatment strategy.

1. Introduction

Graft-versus host disease (GVHD) is characterised by an attack of host organs by donor-derived lymphocytes, and remains as one of the serious complications following haematopoietic stem/progenitor cell transplantation (HSCT). GVHD is classified into acute (aGVHD) and chronic (cGVHD) forms according to the time of disease onset. Recently, distinct mechanisms of pathogenesis between these two forms of GVHD have been reported [1–3]. Nevertheless, the pathophysiology of cGVHD at a molecular level is not well-understood, and studies that directly compared cGVHD with aGVHD using the same donor cell source are few.

Allogeneic mouse models have been developed to investigate acute and chronic GVHD [4–10]. These models supported clarification of the critical roles of T cells as well as donor- and host-derived antigen presenting cells in GVHD. Furthermore, Lockridge et al. described cGVHD in a bone marrow-liver-thymus (BLT) model of humanised NOD/SCID/Il2rgKO (NSG) mice engrafted with human fetal thymic and liver tissue under the renal capsule and injected with HSPCs [11]. Sonntag et al. reported that two out of 15 NSG recipients of human CD34+ haematopoietic stem/progenitor cells (HSPCs) showed cGVHD-like changes at 6–7 months post-transplantation [12]. While these xeno-transplantation models are important milestones in the development of humanised mouse models of in vivo cGVHD, they lacked appropriate humanised microenvironment in the recipient mice. In particular, we focused on human IL-6 signaling, since IL-6 gene polymorphism is associated with the development of cGVHD and anti-human IL-6 receptor monoclonal antibody (Tocilizumab) has shown some benefit in steroid-refractory cGVHD patients [13,14].

Here we present a humanised mouse model for cGVHD through transplantation of human cord blood (CB)-derived HSPCs without implantation of human fetal tissues in human IL-6 expressing NSG mice (hIL-6 Tg NSG). During long-term observation, these cGVHD humanised mice showed cGVHD-like changes in multiple target organs including skin, lung and liver. In addition, we created a humanised mouse model for aGVHD by transplantation of human CB-derived CD34− mature blood and immune cells in NSG mice. Comparison of these two humanised mouse models demonstrated the unique role of macrophages in cGVHD pathogenesis. Moreover, we identified differentially expressed genes in human T cells associated with cGVHD and aGVHD humanised mice. These findings suggest that treatment strategies directed against macrophages as well as specific target molecules associated with pathogenic T cells should be considered as a future therapy for steroid-refractory GVHD.

2. Materials and methods

2.1. Human samples

CB samples were obtained from the Tokai and the Chubu Cord Blood Bank under written informed consent. Peripheral blood (PB) samples were obtained from patients with cGVHD and non-GVHD HSCT recipient at Toranomon Hospital under written informed consent. All experiments were performed with authorisation from the Institutional Review Board for Human Research at RIKEN and were conducted according to the principles expressed in the Declaration of Helsinki.

2.2. Mice

Human *IL-6* Transgenic NSG mice (hIL-6 Tg NSG) were generated by pronuclear microinjection of BAC clone CTD-2594 N23 (GRCh37/hg19 chromosome7 22,724,723–22,964,038; BAC1), or RP11-692 K8 (GRCh37/hg19 chromosome7 22,320,340–22,505,348; BAC2) followed by backcrossing of the transgene >5 generations using a marker-assisted selection protocol from the original C57BL/6 strain onto NOD. Cg-*Prkdc*^{scid}*IL2rg*^{tm1Wjl} (NSG) mice [15]. The copy numbers of the BAC transgene were estimated by quantitative PCR of chloramphenicol-resistance gene in a BAC vector using a mouse endogenous gene (*RAVER2*) as an internal copy-number reference. All mice were bred and maintained under SPF conditions at the animal facility of RIKEN IMS according to guidelines established and approved by the Institutional Animal Committees at RIKEN.

2.3. Purification and transplantation of human cord blood cells

Human CD34+ cells enriched using immune-magnetic beads (130–046-703, Miltenyi Biotec) were used to isolate 7AAD−Lin−CD34+−CD38− or 7AAD−Lin−CD34+CD38−CD45RA− human HSPCs using FACSAria or FACSAria III (BD Biosciences). CB CD34− cells prepared by immune-magnetic microbeads (130–050-1014, Miltenyi Biotec) were used to isolate CB CD34−CD3+ cells using FACSAria. Non-Tg NSG and hIL-6 Tg NSG newborns were sublethally irradiated at 150 cGy total body irradiation using a ¹³⁷Cs-source irradiator followed by intravenous injection via the facial vein. To create cGVHD humanised mice, 1.7×10^3 to 4.5×10^4 HSPCs were transplanted. To create aGVHD humanised mice, 10^5 to 10^6 CD34− or CD34−CD3+ cells were transplanted. To create non-Tg NSG humanised mice, 7.2×10^3 to 4.2×10^5 HSPCs were transplanted. When recipients became moribund (reduced activity or tachypnea), these mice were euthanised and analysed. Non-Tg NSG humanised mice were euthanised concomitantly as controls. Antibodies used for flow cytometric analysis and cell sorting are listed in Supplementary materials and methods.

2.4. RNA-seq analysis

Total RNA was extracted from human T cells and mouse keratinocytes obtained from hIL-6 Tg NSG humanised mice (n = 5), acute GVHD humanised mice (n = 2), non-Tg NSG humanised mice (n = 2), and non-transplanted non-Tg NSG control mice (n = 3) using Trizol (ThermoFisher Scientific). RNA sequencing data are deposited in the National Bioscience Database Center. RNA-seq libraries were prepared using an NEBNext Ultra RNA Library Prep Kit for Illumina (New England Biolabs) according to the manufacturer's protocol and were sequenced using a HiSeq1500 DNA sequencer (Illumina single

---

Fig. 1. Reconstitution of human immunity in hIL-6 Tg NSG mice. (a) Representative flow cytometry plots of a hIL-6 Tg NSG humanised mouse (IL6#1–1) demonstrating the engraftment of human CD19+ B cells, CD33+ myeloid cells, CD3+ T cells, and CD56+ NK cells in BM and spleen. (b) Representative flow cytometry plots showing splenic Treg subsets in a hIL-6 Tg NSG humanised mouse (IL6#1–1). Foxp3+ Tregs are classified into CD45RA+Foxp3^{lo} naïve Tregs (I), CD45RA−Foxp3^{hi} effector Tregs (II), and CD45RA−Foxp3^{lo} non-Tregs (III). (c) Frequency of Foxp3+ Tregs in the spleen are lower in hIL-6 Tg NSG humanised mice (NSG: n = 11, IL-6: n = 14), with significant reduction in naïve Tregs and effector Tregs (NSG: n = 11, IL-6: n = 7) (*$p = 0.0004$, **$p = 0.02$, ***$p = 0.03$). Error bars represent mean ± SEM. (d) T cell-dominant engraftment was found in the skin of hIL-6 Tg NSG humanised mouse as shown by representative flow cytometry plot (IL6#1-1).
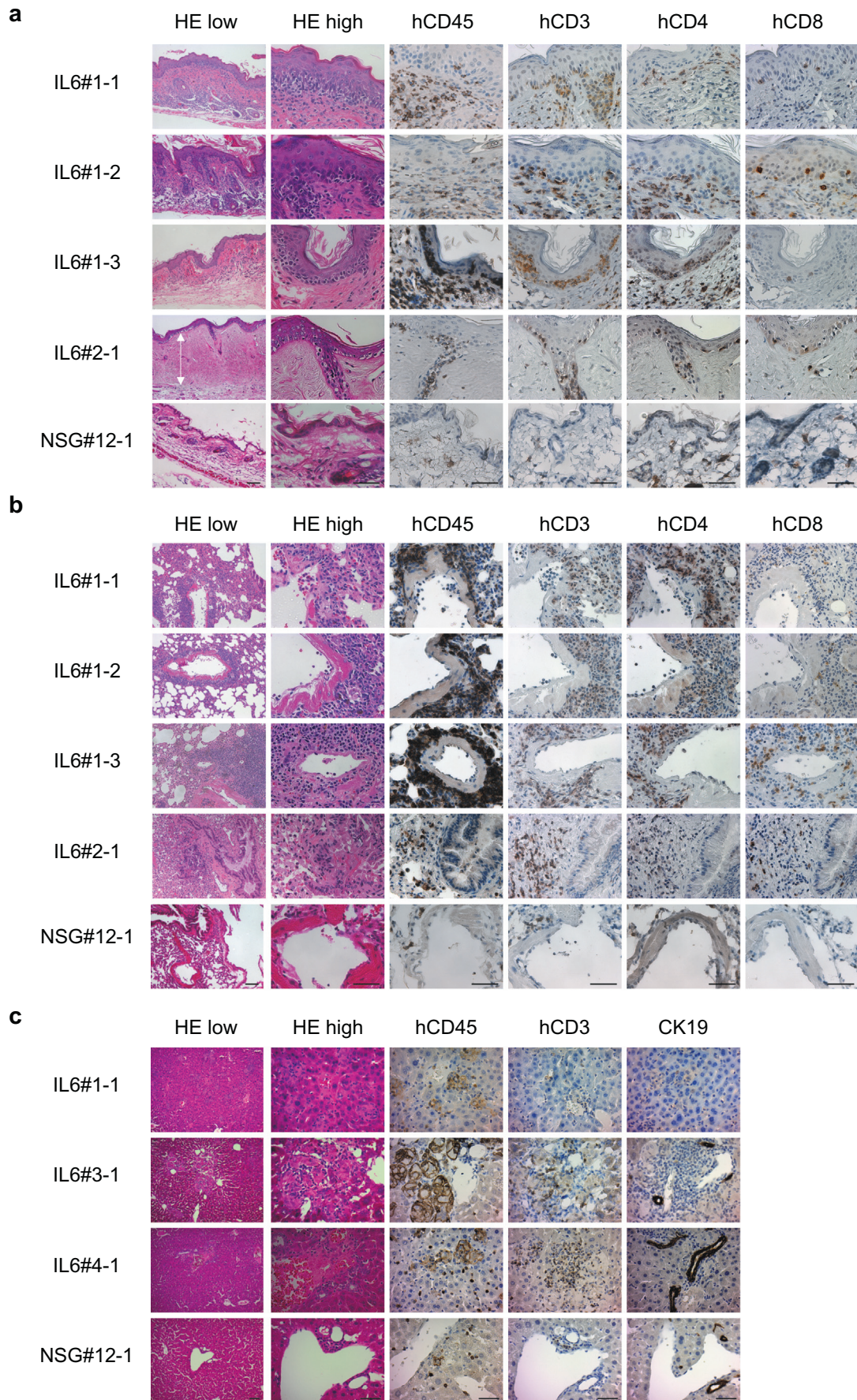
read, 50 bp). The sequence reads were mapped to mouse genome (NCBI version 37) or human genome (NCBI version 19) using TopHat2 (version 2.0.8) and bowtie2 (version 2.1.0) with default parameters and gene annotation was provided by the NCBI RefSeq. The transcript abundances were estimated using Cufflinks (version 2.1.1). Cufflinks was run with the same reference annotation with TopHat2 to generate FPKM (fragments per kilobase per million mapped reads) values for known gene models.

2.5. Transcription factor (TF) enrichment analysis

Enrichment analysis to evaluate effect of a TF on their binding target genes was performed as described previously [16]. Briefly, we compared the mean fold changes of gene expression of target genes of a TF against that of the background (whole genes). To consider heterogeneous frequencies of TF binding among target genes, we used a weighted *t*-test procedure into a parametric gene set enrichment analysis. The frequency of binding of a TF to their target genes was evaluated based on the numerous high-throughput chromatin immunoprecipitation (ChIP) experiments obtained from the gene expression omnibus database (GEO, www.ncbi.nlm.nih.gov/geo/). We used the weighted *t*-statistic as an enrichment score indicating the relative activity of a TF.

2.6. TCR sequencing

Total RNA was extracted from human T cells in hIL-6 Tg NSG humanised mice and acute GVHD humanised mice using Trizol (ThermoFisher Scientific). TCR-seq libraries were prepared using a SMARTer Human TCR a/b Profiling Kit (Clontech Laboratories, Inc.) according to the manufacturer's protocols and were sequenced on a Miseq DNA sequencer (Illumina). The human TCR repertoires were analysed using MiXCR [17].

2.7. Measurement of human cytokine /chemokine levels

Plasma cytokine/chemokine levels in humanised mice and patient samples were measured using the Bio-Plex system (Bio-Rad) with Bio-Plex Human Cytokine 27-Plex and 21-Plex Assay kits (Bio-Rad).

2.8. Statistical analysis

The numerical data are presented as means $\pm$ SEM. Statistical analyses (two-tailed *t*-tests and one-way ANOVA with Bonferroni post-test) were performed using Microsoft Excel. The differences were determined by two-tailed *t*-tests unless otherwise indicated. *P* value <.05 was considered statistically significant. Statistics for Kaplan-Meier analysis were obtained using EZR (Saitama Medical Center, Jichi Medical University, Saitama, Japan), which is a graphical user interface for R (The R Foundation for Statistical Computing, Vienna, Austria) [18].

3. Results

3.1. hIL-6 Tg NSG humanised mice transplanted with human HSPCs develop cGVHD-like changes

We created human *IL6* transgenic NSG mice (hIL-6 Tg NSG) by microinjecting a bacterial artificial chromosome (BAC) containing the human *IL6* gene (clone: 2594 N23 or 692 K8) into C57BL/6 mice and backcrossing onto the NSG background. The BAC transgene was stably propagated in a Mendelian inheritance mode and their copy numbers in mouse clones BAC3 and BAC32 were estimated to be 2.0 copies and 2.9 copies per haploid genome on average of triplicated measurements, respectively. Plasma hIL-6 levels in hIL-6 Tg NSG mice were elevated at baseline (IL-6, $n = 2$: IL-6#1 63.4 pg/ml, IL-6#2 60.7 pg/ml) while non-transgenic NSG mice showed background levels of human IL-6 in plasma (NSG, $n = 2$: NSG#1 0.5 pg/ml, NSG#2 0.6 pg/ml).

To create cGVHD humanised mouse, we transplanted human CB-derived HPSCs into sublethally-irradiated hIL-6 Tg NSG newborns. At 20 to 43 weeks post-transplantation, all hIL-6 Tg NSG humanised mice developed signs of weakness including ruffled fur, anemia and reduced mobility ($n = 58$). In 22 out of 58 these mice, we found macroscopic skin lesions consistent with skin cGVHD. We examined human immuno-haematopoietic reconstitution in 18 out of 22 and found long-term multi-lineage engraftment of human CD19$^+$ B cells, CD33$^+$ myeloid cells, CD3$^+$ T cells, and CD56$^+$ natural killer cells in the bone marrow (BM) and spleen of hIL-6 Tg NSG mice (Representative flow cytometry plots shown in Fig. 1a, Table S1). Engrafted human T cells were predominantly TCR$\alpha\beta^+$ T cells. Interestingly, the frequency of Foxp3$^+$ Tregs was lower in hIL-6 Tg NSG humanised mice (hIL-6 Tg, $n = 14$: 5.7 $\pm$ 0.9%, non-Tg NSG, $n = 11$: 10.5 $\pm$ 0.6%, $p = .0004$; Fig. 1b). Analysis of Foxp3+ Treg subsets CD45RA$^+$Foxp3^{lo} naïve Tregs (nTregs), CD45RA$^-$Foxp3^{hi} effector Tregs (eTregs) and CD45RA$^-$Foxp3^{lo} non-Tregs (non-Tregs) (Representative flow cytometry plots in Fig. 1b) [19] showed reduction of both naïve ($p = 0.02$) and effector ($p = 0.03$) fractions in the spleen of hIL-6 Tg NSG humanised mice (non-Tg NSG, $n = 11$: nTregs 0.5 $\pm$ 0.1%, eTregs 3.9 $\pm$ 0.6%; IL-6, $n = 7$, nTregs 0.1 $\pm$ 0.04%, eTregs 1.8 $\pm$ 0.6%; Fig. 1c).

We performed histological examination of the skin, lung and liver in hIL-6 NSG humanised mice with and without macroscopic skin lesions. We found infiltration of human T cells in the macroscopically-apparent skin lesions in all 14 mice examined (Representative flow cytometry plots shown in Fig. 1d). We performed histological examination of the skin in 27 mice (with macroscopic skin lesions: $n = 14$; no macroscopic skin lesions: $n = 13$). In 21 of 27, we found epidermal thickening, interface dermatitis (vacuolar changes beneath basal keratinocytes), reduced numbers of adipocytes, reduced numbers of hair follicles and infiltration of human CD4$^+$ and CD8$^+$ T cells in epidermis and dermis (Fig. 2a). These abnormalities were present even in 7 of 13 recipients with no macroscopic skin lesions. In three out of 14, sclerotic changes were present in the dermis. Altered expression of cytokeratins may trigger or exacerbate inflammatory skin diseases [20]. We found ectopic expression of cytokeratin 17 and reduced expression of cytokeratin 13 in skin sections of hIL-6 Tg NSG humanised mice, suggesting possible role of these cytoskeletal filaments in skin pathology [21,22] (Fig. S1). In 19 of 27 examined, hIL-6 Tg NSG humanised mice lungs showed infiltration of human T cells in peri-vascular areas, obstruction of bronchioles, and peri-bronchiolar areas with fibrotic changes (Fig. 2b). In 13 of 21 mice examined, we found reduction of cytokeratin 19-positive small bile ducts in the liver and obstruction of portal triads presumably as a consequence of chronic inflammation (Fig. 2c). These histopathological findings are consistent with cGVHD in skin, lung and liver of mice with macroscopically normal skin as well as those with macroscopically appreciable skin lesions. Notably, cGVHD-like changes were found in the majority of mice examined whether or not macroscopic skin lesions were present. These changes were not found in non-Tg NSG humanised mice and untransplanted NSG and hIL-6 Tg mice (Fig. 2 and Fig. S2) [23].

Fig. 2. Histological analysis of cGVHD humanised mice. Histological analysis of (a) skin, (b) lung and (c) liver from hIL-6 Tg NSG humanised mice with a hIL-6 non-Tg NSG humanised mouse as control. (a) H&E and immunohistochemical staining is consistent with interface dermatitis with epidermal thickening associated with infiltration of CD4$^+$ and CD8$^+$ T cells in cGVHD humanised mice. White arrow shows sclerotic and thickened upper dermis (IL6#2-1). (b) Pulmonary sections of the same recipients show infiltration of CD4$^+$ T and CD8$^+$ T cells. (c) Infiltration of human CD45$^+$ leucocytes including CD3$^+$ T cells is detected in the liver of cGVHD humanised mice. In contrast, a non-Tg NSG humanised mouse (NSG#12-1) shows normal skin, lung and liver histology. Scale bars: Low magnification 100 μm; high magnification 50 μm.
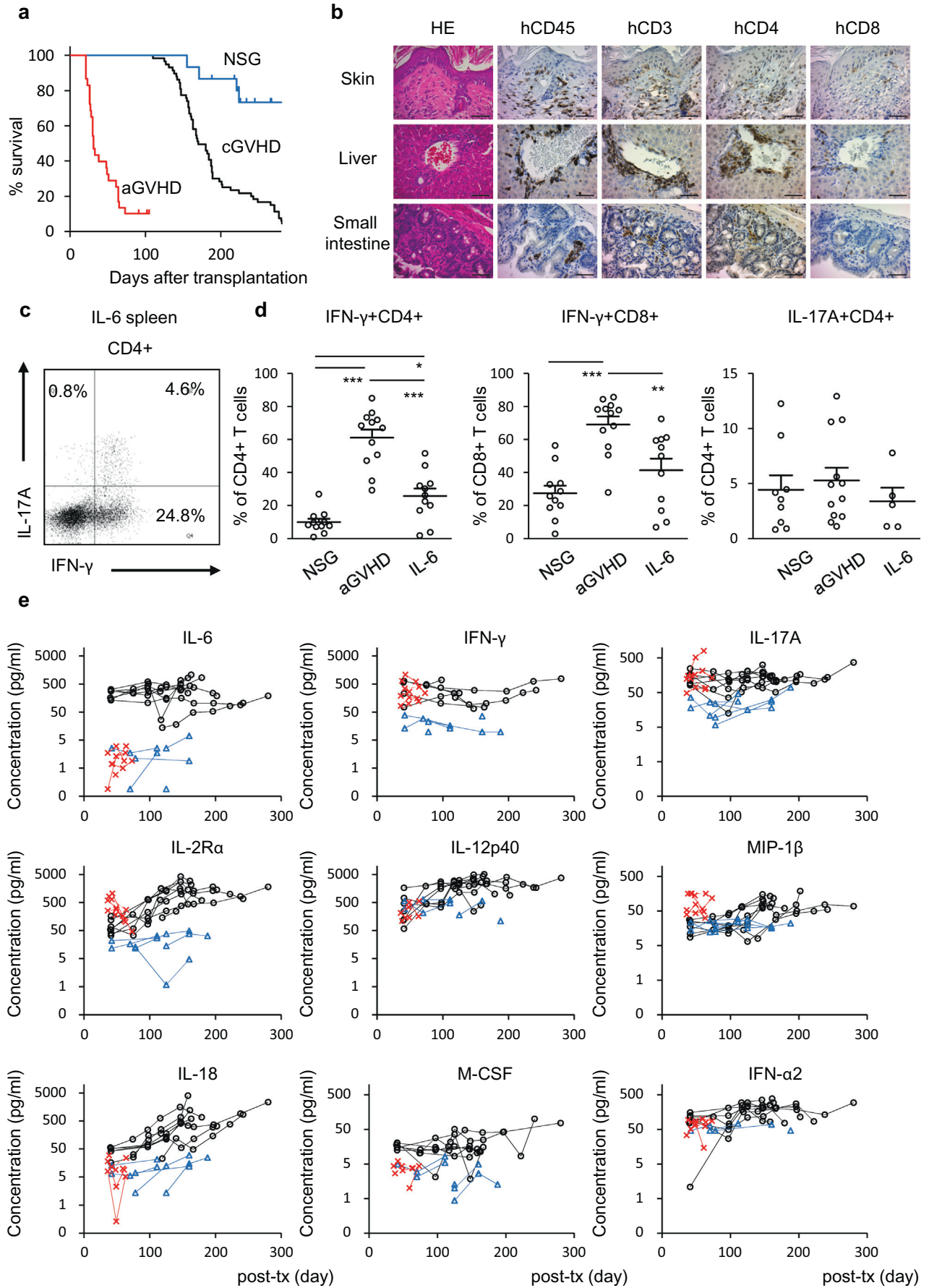
3.2. Both cGVHD and aGVHD humanised mice show T cell activation

Although damage to host organs mediated by activated T cells is found in both aGVHD and cGVHD, distinct mechanisms underlying the activation of donor T cells in these two clinical entities are not fully understood. To evaluate the differences between aGVHD and cGVHD, we created an aGVHD humanised mouse model by transplanting human CB-derived CD34-negative mature haematopoietic cells ($n = 16$) or CD34$^-$CD3$^+$ T cells ($n = 10$) into non-Tg NSG newborns (Table S2). CB-derived CD34-negative cells contain T cells, B cells, myeloid cells and NK cells (CD34-cells, n = 10: CD3$^+$ cells 26.8 ± 3.6%; CD19$^+$ cells 22.3 ± 5.4%; CD33$^+$ cells 33.4 ± 5.9%; CD56$^+$ cells 14.3 ± 3.4%, Fig. S3). Unlike hIL-6 Tg NSG cGVHD humanised mice, onset of disease was rapid in aGVHD humanised mice with 23 of 26 recipients becoming moribund within 73 days of transplantation. Early onset of GVHD in these recipients led to reduced survival compared with cGVHD humanised mice (Fig. 3a). Vast majority of human CD45$^+$ leukocytes in the PB, spleen, liver, lung, gastrointestinal tract and skin of the aGVHD humanised mice were CD3$^+$ T cells (Table S2 and Fig. S4a). Nine of 26 recipients developed macroscopically-apparent skin lesions. Histological analysis of the skin showed epidermal thickening with human T cell infiltration and ectopic cytokeratin 17 expression in the epidermis [21,22] (Fig. 3b, Fig. S1). Infiltration of human T cells was also observed in the liver and small intestine, major target organs of clinical aGVHD (Fig. S4a, Fig. 3b). Histologically, sclerotic changes and reduction of bile ducts were absent in aGVHD humanised mice, in contrast to hIL-6 Tg NSG cGVHD humanised mice (Fig. 3b and Fig. S4b).

To understand the differences in mechanisms of immune-mediated pathogenesis in cGVHD and aGVHD, we evaluated function of immune cells in these two models. While the frequencies of CD4+ and CD8+ T cells were similar in BM and spleen of cGVHD and aGVHD humanised mice, frequencies of IFN-γ producing cells among splenic CD4$^+$ T cells (NSG, $n = 11$: CD4$^+$IFN-γ$^+$ 9.9 ± 2.1%; aGVHD $n = 12$: CD4$^+$IFN-γ$^+$ 61.1 ± 5.0%; IL-6, n = 11: CD4$^+$IFN-γ$^+$ 25.7 ± 4.6%, $p = 0.005$ between NSG and IL-6, $p < 0.0001$ between aGVHD and IL-6, and p < .0001 between NSG and aGVHD), and CD8$^+$ T cells (NSG, n = 11: CD8$^+$IFN-γ$^+$ 27.3 ± 4.7%; aGVHD, n = 12: CD8$^+$IFN-γ$^+$ 69.1 ± 4.9%; IL-6, n = 11: CD8$^+$IFN-γ$^+$ 41.4 ± 7.0%, $p = 0.004$ between aGVHD and IL-6 and p < 0.0001 between NSG and aGVHD) were higher in aGVHD humanised mice (Fig. 3c–d, Fig. S5a). Frequencies of IL-17A producing cells were similar among the three groups (NSG, $n = 9$: CD4$^+$IL17A$^+$ 4.4 ± 1.3%; aGVHD, n = 12: CD4$^+$IL17A$^+$ 5.3 ± 1.2%; IL-6, $n = 5$: CD4$^+$IL17A$^+$ 3.4 ± 1.2%, Fig. 3c, d). Mouse and human CD4$^+$ T cells that express specific chemokine receptors are known to produce specific sets of cytokines [24] [24]. Consistent with increased frequencies of IFN-γ$^+$CD4$^+$ T cells, both aGVHD and hIL-6 Tg NSG cGVHD humanised mice showed higher frequencies of CXCR3-expressing human CD4$^+$ T cells compared with non-Tg humanised mice while the frequencies of CCR6-expressing human CD4$^+$ T cells were similar (Fig. S5b–d). Thus, although both acute and chronic GVHD showed T cell activation, distinct histology, infiltrating immune cell subsets, and the frequencies of IFN-γ production by activated T cells were observed between acute and chronic GVHD model mice (Table S3).

3.3. Monocytes/macrophages are activated in the lung and liver of cGVHD mice

Previously, certain cytokines and chemokines have been reported as diagnostic and prognostic biomarkers of both acute and chronic GVHD
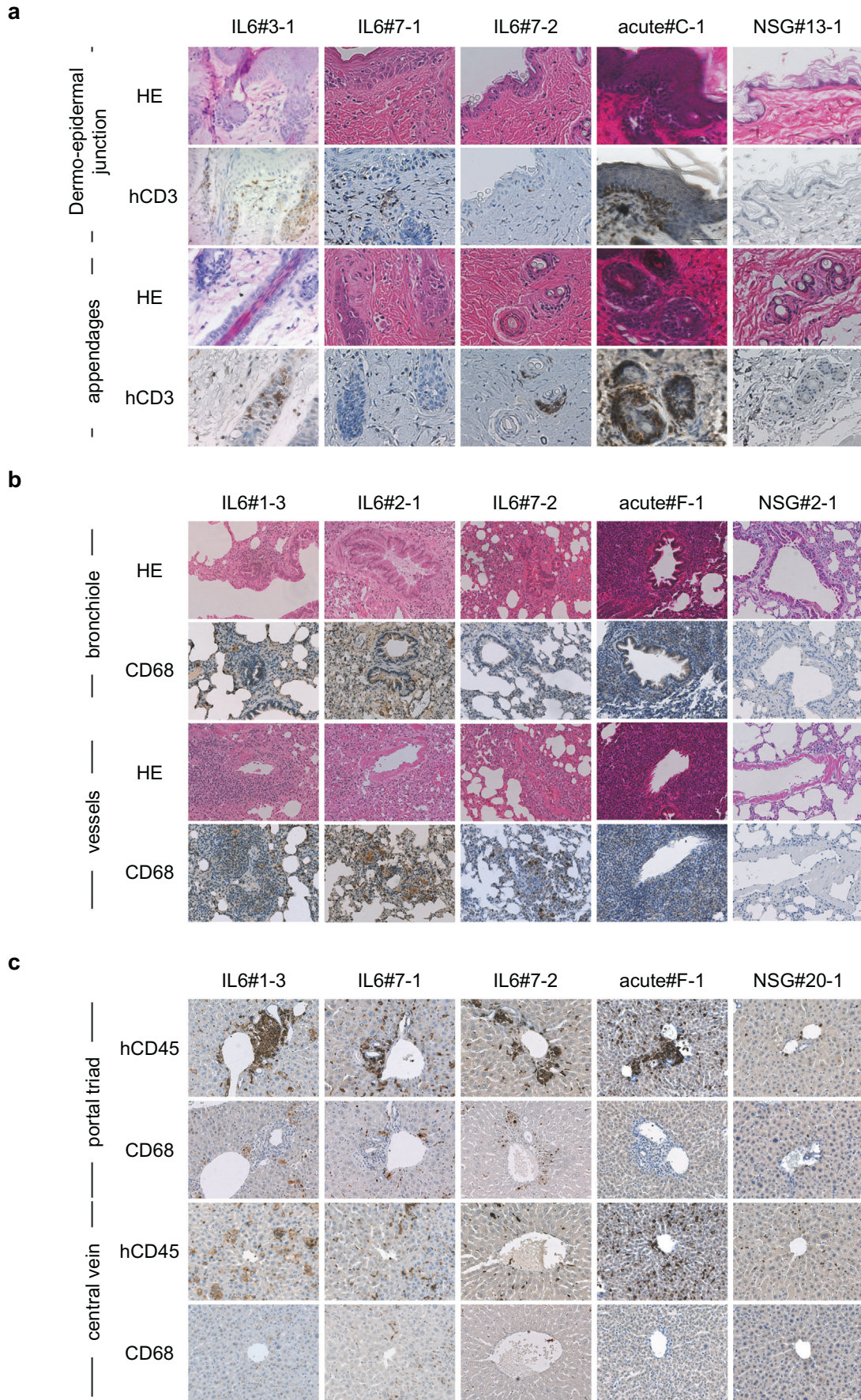
[25,26]. In cGVHD humanised mouse plasma, in addition to T cell-associated soluble factors (e.g., IFN-γ, IL-17A, IL-2Rα), myeloid cell- or stromal cell-associated factors MIP-1β, IL-6, IL-12/23-p40, IL-18, IFN-α2, and M-CSF[27,28] were elevated (Fig. 3e). Since human T cell reconstitution in PB of these mice were scant at 40 days post-transplantation (Fig. S6a-b), macrophages activated by hIL-6 present at high levels likely contributes to the production of these cytokines and chemokines. Consistent with these findings, plasma concentration of myeloid-associated cytokines in cGVHD patients showed higher levels of macrophage-associated cytokines and chemokines MIP-1β, IL-18, M-CSF, and IFN-α2 compared with a post-HSCT patient without GVHD, suggesting macrophage activation may be one of the mechanisms contributing to cGVHD pathogenesis (cGVHD patients, $n = 3$: MIP-1β 109.8 ± 14.2 pg/ml, IL-18121.3 ± 6.7 pg/ml, M-CSF 21.5 ± 0.8 pg/ml, IFN-α2 81.3 ± 14.1 pg/ml; patient with no GVHD, $n = 1$: MIP-1β 30.8 pg/ml, IL-18 83.5 pg/ml, M-CSF below our-of-range, IFN-α2 15.6 pg/ml).

Next, we confirmed in situ macrophage activation in cGVHD humanised mice (Fig. 4). As shown in Fig. 4a, cGVHD mice showed sclerotic changes in the dermis, epidermal hyperkeratosis, reduction of adipocytes and appendages. On the other hand, intensive lymphocytic infiltration into dermo-epidermal junction or appendages were characteristics of aGVHD mice. In the lung and liver of cGVHD humanised mice, we detected prominent infiltration of CD68$^+$ macrophages (Fig. 4b–c and Fig. S6c–d). These CD68$^+$ cells were larger in cGVHD humanised mice compared with those in aGVHD humanised mice, suggesting that human macrophages were activated in cGVHD mice. In cGVHD humanised mouse lungs, we also found infiltration of enlarged macrophages in the peri-bronchiolar and peri-vascular areas with obstructed bronchioles surrounded by both CD3$^+$ T cells and CD68$^+$ macrophages. In contrast, peri-bronchiolar and peri-vascular infiltration in aGVHD humanised mice was CD3$^+$ T cell-dominant, containing scant macrophages (Fig. S7). Among 27 mice examined, 19 cGVHD mice showed severe macrophage infiltration in the lung. In contrast, CD68$^+$ cells in non-Tg NSG humanised mice and aGVHD humanised mice were scant and did not appear to proliferate in the organ (Fig. 4b, Fig. S7). Likewise, infiltration of enlarged macrophages in the portal triad region was characteristic liver histopathology in cGVHD humanised mice, in contrast to dominant T cell infiltration in the liver of aGVHD humanised mice (Fig. 3b, Fig. 4c and Fig. S4b). Macrophage infiltration was also detected in the lung and liver of cGVHD humanised mice without skin involvement, which might account for decreased activity and shortened survival (Fig. S8). Together, these findings in cGVHD humanised mice suggest that co-activation of human macrophages and T cells may underlie pathogenesis of cGVHD while aGVHD results from activated human T cells through recognition of host tissue as non-self.

3.4. Gene expression signatures of human T cells and mouse keratinocytes in acute and chronic GVHD humanised mice

Next, we examined the transcriptome of cGVHD and aGVHD humanised mice to understand the distinct pathophysiology of acute and chronic GVHD at the level of gene expression. To do so, we isolated hCD45$^+$CD3$^+$ skin T cells, hCD45$^+$CD3$^+$TCRab$^+$CD4$^+$ spleen CD4$^+$ T cells, and hCD45$^+$CD3$^+$TCRab$^+$CD8$^+$ spleen CD8$^+$ T cells from acute and chronic GVHD humanised mice and non-Tg NSG humanised mice (Fig. S9a-b). In addition, we isolated mCD45$^-$hCD45$^-$E-cadherin$^+$ mouse skin keratinocytes from cGVHD humanised mice, aGVHD

humanised mice, and non-transplanted control non-Tg NSG mice to an-alyse altered gene expression in mouse keratinocytes during the devel-opment of GVHD (Fig. S9a). When we compared gene expression signatures of spleen T cells from aGVHD and cGVHD humanised mice to those of non-Tg NSG humanised mice, 1121 and 1022 genes were found to be differently expressed in aGVHD and cGVHD, respectively. Among them, 470 genes were shared between aGVHD and cGVHD mice (Fig. 5a). In aGVHD humanised mice, expression of *VDR* in skin T cells and *CCL4*, *TNFSF9,* and *BHLHE40* in spleen and skin T cells were up-regulated compared with cGVHD humanised mice, reflecting activated status of T cells.[29–31] Among differentially-expressed genes, we found higher expression of *CCL3* in skin T cells of aGVHD humanised mice, while *CLU*, a gene associated with macrophage activation, [32,33], was upregulated in those of cGVHD humanised mice (Fig. 5b). Through tran-scription factor (TF) enrichment analysis that evaluates the effects of TFs on gene expression [16], we identified significantly higher expression of target genes of multiple TFs in cGVHD humanised mouse skin T cells (Fig. 5c, d). Among them were target genes of *TRRAP*, *KAT2B*, and *SRBP1* associated with phosphatidylinositol-3-kinase (PI3K) signaling pathway [34–36]. In addition, we found enrichment of genes whose ex-pression is potentially regulated by TFs *CTBP1* and *ZNF143* in cGVHD humanised mouse skin T cells (Fig. 5d). These two TFs were reported to be involved in epithelial-mesenchymal transition (EMT) [37,38]. EMT, triggered by aberrant TGF-β/SMAD signaling, is thought to con-tribute to the development of systemic sclerosis and bronchiolitis obliterans after lung transplantation, both sharing pathological findings with cGVHD [39,40]. Consistent with these findings, expression of target genes of *NR2C2* and *KDM5A*, associated with the TGF-β/SMAD signaling pathway, were enriched in cGVHD humanised mouse skin T cells [41–44] (Fig. 5d).

When comparing transcriptomic signatures of keratinocytes of aGVHD humanised mice, cGVHD humanised mice and untransplanted non-Tg NSG control mice (Fig. 5e-h), skin keratinocytes of cGVHD humanised mice showed similarities with autoimmune diseases such as type 1 diabetes mellitus, rheumatoid arthritis, and systemic lupus er-ythematosus (Fig. 5g). Higher expression of binding-target genes of *Irf1*, *Irf8* and *Junb* associated with activation of macrophages and chronic in-flammation[45,46] was also confirmed in keratinocytes of cGVHD mice (Fig. 5h). We further evaluated mRNA expression of multiple organs in-cluding brain, salivary gland, liver, lung, spleen and skin (obtained from the back, right leg and left leg) of a cGVHD humanised mouse by quantitative PCR (Fig. S9c). In addition to genes downstream of IL-6 sig-naling, *JAK2* and *STAT3*, several genes involved in production of inflam-matory molecules such as *IFNG*, *TGFB1*, *TNFSF10*, and *TLR2* and activation markers for macrophages, *MYD88* and *NFκB1*, were also upregulated. From transcriptomic analyses, T cells of cGVHD humanised mice might play pathogenic roles in not only cytotoxicity but also fibrotic change through accelerating TGF-β/SMAD signaling pathway, promoting EMT, and macrophage activation.

3.5. TCR repertoire analyses of cGVHD and aGVHD humanised mice

We analysed the repertoire of alpha and beta loci of TCR genes (TRA and TRB) in human T cells isolated from PB and spleen of aGVHD (n = 4) and cGVHD humanised mice (n = 3). While both possessed skewed TRA and TRB repertoires in the skin and spleen, aGVHD mice appeared to have more skewed repertoire (Fig. 6a). Therefore, we next examined whether these expanded T cell clones are present among target organs of aGVHD. From TRA and TRB repertoire analyses of CD4⁺ and CD8⁺ T cells of an aGVHD humanised mouse, we found dominant clones were shared among spleen, lung, and liver (Fig. 6b-c). These findings suggest

that aGVHD might be triggered by clonal expansion of specific T cell clones that recognise host-derived common target antigens, and direct cytotoxicity of expanded T cells may be the major cause of tissue damage.

4. Discussion

In this study, we report the creation of cGVHD humanised mice through engraftment of human HSPCs in hIL-6 Tg NSG recipients. These humanised mice develop manifestations consistent with cGVHD involving the skin, lung and liver, including interface dermatitis, peri-bronchiolar vasculitis, bronchiolitis obliterans and reduced numbers of bile ducts associated with infiltration of human T cells and macrophages in the affected areas [23,47]. These findings were unique to cGVHD humanised mice, as affected skin, lung and liver of aGVHD humanised mice showed predominantly T cell infiltration.

Several cGVHD mouse models have been reported to date [4–12]. Unlike these models, in our humanised mouse model, cGVHD was in-duced de novo through in vivo development of pathologic immune cells from human CD34⁺CD38⁻ or CD34⁺CD38⁻CD45RA⁻ HSPCs in re-cipient mice that overexpress human IL-6. IL-6 has been implicated in the pathogenesis of post-transplant cGVHD through studies showing the association of IL-6 gene polymorphism with the development of cGVHD [13] and Drobyski et al. reported the beneficial effect of anti-human IL-6 receptor monoclonal antibody (Tocilizumab) in steroid-refractory cGVHD [14]. To directly compare acute and chronic GVHD arising from the same human haematopoietic source, we further cre-ated an aGVHD humanised mouse model by injecting human CB CD34⁻ mature haematopoietic cells into NSG newborns. In line with previous aGVHD humanised mouse models created by injection of human PB mononuclear cells 48–52, both CD4⁺ and CD8⁺ T cells were detected in the target organs of aGVHD.

In both cGVHD and aGVHD humanised mice, predominantly CD45RA⁺CD45RO⁻ naïve CB T cells became strongly activated in vivo as shown by the elevation of plasma cytokine/chemokines such as IL-2Rα, IFN-γ, and MIP-1β. Although activation of T cells is a hallmark of both aGVHD and cGVHD, our humanised mouse models demonstrated distinct histopathology, cytokine/chemokine profiles and transcriptome in cGVHD, showing that activated macrophages cooperate with T cells in cGVHD pathogenesis. In line with this observation, clinical cGVHD samples also showed elevation of cytokines/chemokines associated with macrophage development and activation. In contrast to aGVHD where dominant oligo-clonal T cells against shared epitopes were pres-ent in multiple target organs, interaction of activated macrophages and T cells in the setting of excess IL-6 and reduced immune-regulatory function may explain broader T cell repertoire in cGVHD.

Importance of innate immunity in triggering aberrant immune reac-tion has been reported through GWAS using 492 donor-recipient paired samples from HLA-matched sibling HSCT recipients [53]. Macrophage activation in involved organs and expression of *CLU* and binding target genes of *NR2C2,* associated with macrophage activation/recruitment, [32,33,41] by T cells infiltrating the affected skin suggest the role of T cells in recruiting and activating macrophages in cGVHD. In addition to changes at the transcript level, we found elevated production of human IL-12p40, IL-18, M-CSF, IFN-α2 by monocytes/macrophages that may facilitate pathogenesis in cGVHD humanised mice.

In particular, M-CSF and type-1 IFN promote differentiation and maturation of macrophages and are reported to be associated with the development of cGVHD [4,54]. Recently, macrophage activation by M-CSF has been shown to contribute to the development and progres-sion of cGVHD via TGF-β production, fibroblast activation, excess

Fig. 4. Infiltration of human immune cells and histopathology characteristic of acute and chronic GVHD humanised mice. (a-c) Histological sections of cGVHD humanised mice (IL-6: n = 3), an aGVHD humanised mouse (acute: n = 1), and non-Tg NSG humanised mouse (NSG: n = 1). (a) HE and hCD3 stained sections of skin dermo-epidermal junction (top two panels) and skin appendages (bottom two panels) are shown. (b) HE and CD68 stained sections of peri-bronchiolar (top two panels) and peri-vascular (bottom two panels) regions are shown. (c) hCD45 and CD68 stained sections of portal triad (top two panels) and peri-central vein (bottom two panels) regions are shown.
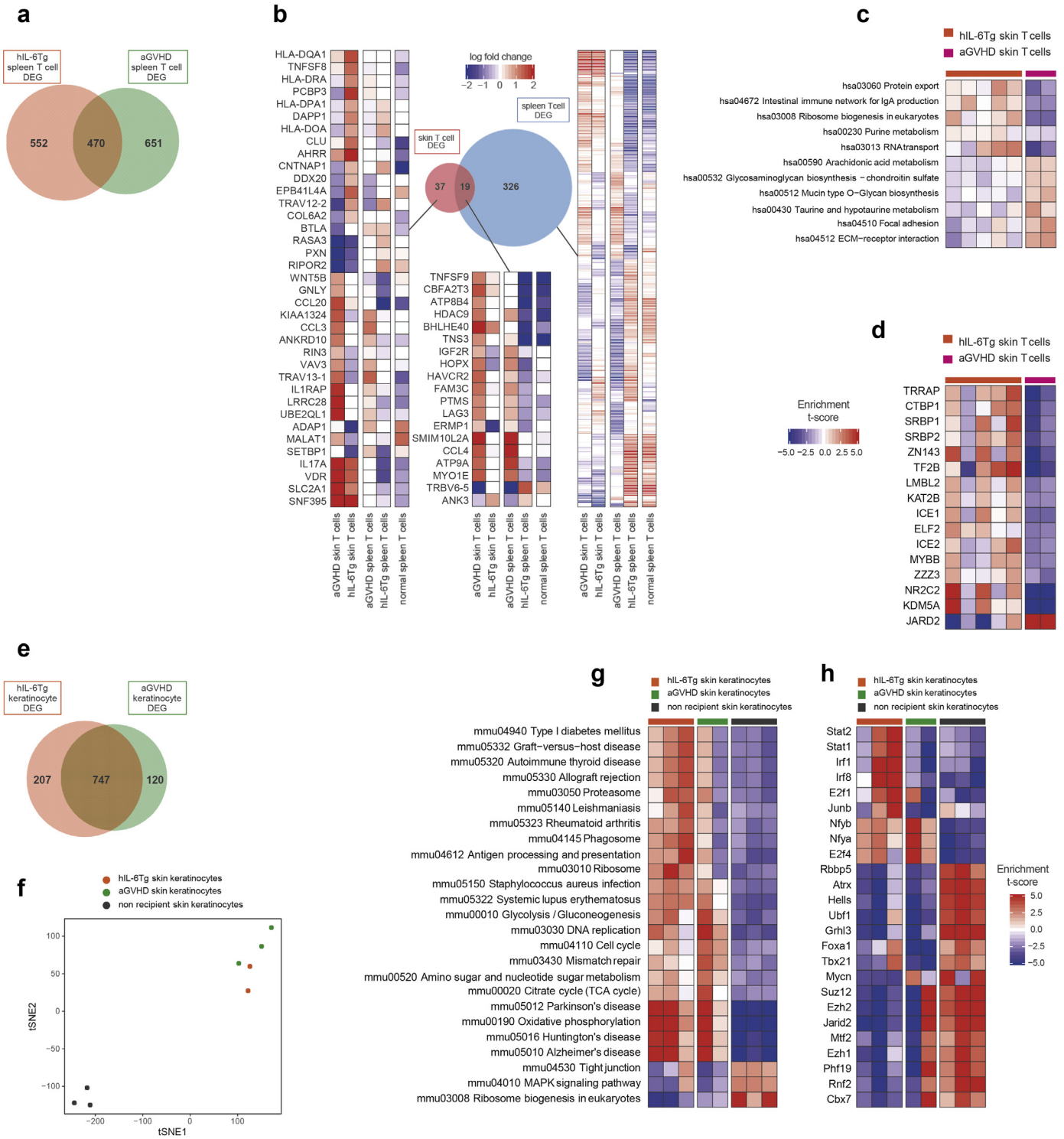
Fig. 5. Gene expression signatures of T cells and keratinocytes in cGVHD and aGVHD humanised mice. (a) Venn diagrams indicating differentially expressed genes in splenic T cells among cGVHD and aGVHD humanised mice. (b) Differentially expressed genes among skin and spleen T cells in acute and chronic GVHD mice and non-Tg NSG humanised mice. (c) KEGG pathway enrichment analysis and (d) transcription factor (TF) enrichment analysis of skin T cells. (e) Venn diagrams indicating differentially expressed genes in skin keratinocytes from cGVHD and aGVHD humanised mice. (f) Dimensionality reduction plot using tSNE. (g) KEGG pathway enrichment analysis and (h) transcription factor (TF) enrichment analysis of skin keratinocytes.

production of extracellular matrix and collagen, and subsequent tissue fibrosis. [2,4]. Consistent with this, inhibition of monocytes and macrophages by pirfenidone ameliorates established cGVHD in mice [6]. While TGF-β activation can lead to immune-suppression through promotion of Treg differentiation, IL-6 has been reported to moderate this effect [55]. Therefore, concurrent elevation of TGF-β and IL-6, may

initiate pathologic changes in cGVHD possibly through macrophage activation. In addition, IL-6 has been shown to switch differentiation of monocytes from dendritic cells to macrophages [56]. Therefore, aberrant expression of IL-6 might disrupt homeostasis of both T cells and myeloid cells. Our findings using the cGVHD humanised mice suggest there are bidirectional and synergistic interactions between activated
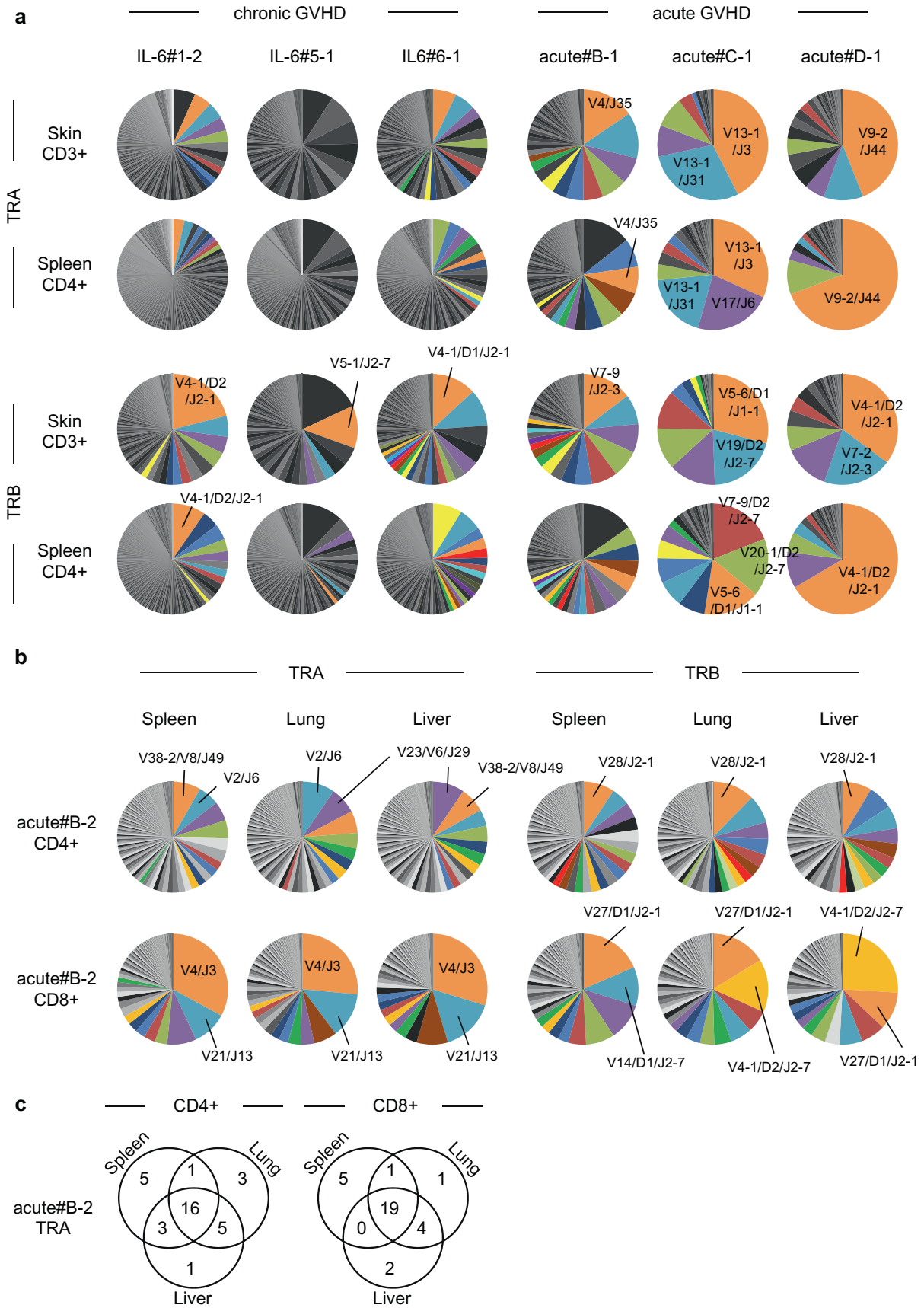
Fig. 6. TCR repertoires in acute and chronic GVHD humanised mice. (a,b) TRA and TRB repertoire of (a) skin T cells and spleen CD4$^+$ T cells from cGVHD humanised mice (n = 3) and (b) spleen, lung and liver CD4$^+$ and CD8$^+$ T cells from aGVHD humanised mice (n = 3). When same clones accounted for >1%, they are shown using the same colour. (c) Venn diagrams show overlap of 25 most frequent clones among spleen, lung, and liver.

T cells and activated macrophages in the setting of elevated IL-6 and suppressed Treg-mediated immune-regulation leading to cGVHD pathogenesis.

Identifying molecular targets against GVHD is critical to reduce therapy-related mortality in stem cell transplantation. Using the cGVHD and aGVHD humanised mice, we identified gene expression signatures defining these conditions both systemically (in the spleen) and locally (in the skin). In aGVHD, certain genes such as *VDR*, *TNFSF9*, and *BHLHE40* were upregulated reflecting T cell activation via TCR stimulation [29–31]. On the other hand, activated human T cells in cGVHD humanised mice showed upregulation of PI3K signaling (TRRAP, KAT2B, and SRBP1), EMT-associated transcripts (CTBP1 and ZNF143), and TGF-β/SMAD signaling (NR2C2 and KDM5A). Since both TGF-β/SMAD signaling and EMT is important in tissue remodeling, these pathways might play important roles in the development of fibrotic lesions in cGVHD and suggest that these pathways may be potential therapeutic targets.

Though recent studies suggested anti-thymocyte globulin as a prophylactic therapy to reduce the frequencies of cGVHD [57], suppression of T cells is problematic in patients with malignancy [58]. While corticosteroids are well-established as first line treatment, there are no widely-accepted second line therapies for cGVHD [59]. In addition to the recent attempt of adoptive Treg transfer or in vivo Treg expansion using low-dose IL-2 [60,61], co-inhibition of activated macrophages and T cells might become a promising therapeutic strategy for cGVHD. The humanised mouse model for cGVHD may serve as a pre-clinical model to assess therapeutic effect against hyper-activated human immune cells in multiple organs.

Supplementary data to this article can be found online at https://doi.org/10.1016/j.ebiom.2019.02.001.

Funding

Author contributions

R.O., H.Y., Y.S., L.D.S., O.O., M.A., H.K., and F.I. designed the study. R.O., M.I., M.T.-M., M.M., Y.N., S.F., and R.S. performed experiments. R.O., E.K., M.I., and F.I. analysed the data. Shinsuke Takagi, K.S., H.Y., S.K. and Shuichi Taniguchi provided resources and put intellectual input. T.W., E.K., and Y.M. performed and analysed genomic data. R.O., Y.S., L.D.S., O.O., M.A., H.K., and F.I. wrote the manuscript. All authors read and approved the final manuscript.

Declaration of interests

The authors declare that they have no competing interests.

References

[1] Blazar BR, Murphy WJ, Abedi M. Advances in graft-versus-host disease biology and therapy. Nat Rev Immunol 2012;12(6):443–58.
[2] MacDonald KP, Blazar BR, Hill GR. Cytokine mediators of chronic graft-versus-host disease. J Clin Invest 2017;127(7):2452–63.
[3] Socie G, Ritz J. Current issues in chronic graft-versus-host disease. Blood 2014;124 (3):374–84.
[4] Alexander KA, Flynn R, Lineburg KE, et al. CSF-1-dependant donor-derived macrophages mediate chronic graft-versus-host disease. J Clin Invest 2014;124(10): 4266–80.
[5] Anderson BE, McNiff JM, Jain D, Blazar BR, Shlomchik WD, Shlomchik MJ. Distinct roles for donor- and host-derived antigen-presenting cells and costimulatory molecules in murine chronic graft-versus-host disease: requirements depend on target organ. Blood 2005;105(5):2227–34.
[6] Du J, Paz K, Flynn R, et al. Pirfenidone ameliorates murine chronic GVHD through inhibition of macrophage infiltration and TGF-beta production. Blood 2017;129(18): 2570–80.
[7] Kaplan DH, Anderson BE, McNiff JM, Jain D, Shlomchik MJ, Shlomchik WD. Target antigens determine graft-versus-host disease phenotype. J Immunol 2004;173(9): 5467–75.
[8] Sakoda Y, Hashimoto D, Asakura S, et al. Donor-derived thymic-dependent T cells cause chronic graft-versus-host disease. Blood 2007;109(4):1756–64.
[9] Schroeder MA, DiPersio JF. Mouse models of graft-versus-host disease: advances and limitations. Dis Model Mech 2011;4(3):318–33.
[10] Zhang Y, Hexner E, Frank D, Emerson SG. CD4+ T cells generated de novo from donor hemopoietic stem cells mediate the evolution from acute to chronic graft-versus-host disease. J Immunol 2007;179(5):3305–14.
[11] Lockridge JL, Zhou Y, Becker YA, et al. Mice engrafted with human fetal thymic tissue and haematopoietic stem cells develop pathology resembling chronic graft-versus-host disease. Biol Blood Marrow Transplant 2013;19(9):1310–22.
[12] Sonntag K, Eckert F, Welker C, et al. Chronic graft-versus-host-disease in CD34(+)-humanised NSG mice is associated with human susceptibility HLA haplotypes for autoimmune disease. J Autoimmun 2015;62:55–66.
[13] Cavet J, Dickinson AM, Norden J, Taylor PR, Jackson GH, Middleton PG. Interferon-gamma and interleukin-6 gene polymorphisms associate with graft-versus-host disease in HLA-matched sibling bone marrow transplantation. Blood 2001;98(5): 1594–600.
[14] Drobyski WR, Pasquini M, Kovatovic K, et al. Tocilizumab for the treatment of steroid refractory graft-versus-host disease. Biol Blood Marrow Transplant 2011;17(12): 1862–8.
[15] Ishikawa F, Yasukawa M, Lyons B, et al. Development of functional human blood and immune systems in NOD/SCID/IL2 receptor {gamma} chain(null) mice. Blood 2005; 106(5):1565–73.
[16] Kawakami E, Nakaoka S, Ohta T, Kitano H. Weighted enrichment method for prediction of transcription regulators from transcriptome and global chromatin immuno-precipitation data. Nucleic Acids Res 2016;44(11):5010–21.
[17] Bolotin DA, Poslavsky S, Mitrophanov I, et al. MiXCR: software for comprehensive adaptive immunity profiling. Nat Methods 2015;12(5):380–1.
[18] Kanda Y. Investigation of the freely available easy-to-use software 'EZR' for medical statistics. Bone Marrow Transplant 2013;48(3):452–8.
[19] Miyara M, Yoshioka Y, Kitoh A, et al. Functional delineation and differentiation dynamics of human CD4+ T cells expressing the FoxP3 transcription factor. Immunity 2009;30(6):899–911.
[20] Vijayaraj P, Sohl G, Magin TM. Keratin transgenic and knockout mice: functional analysis and validation of disease-causing mutations. Methods Mol Biol 2007;360: 203–51.
[21] Al-Refu K, Goodfield M. Hair follicle stem cells in the pathogenesis of the scarring process in cutaneous lupus erythematosus. Autoimmun Rev 2009;8(6):474–7.
[22] Nobusawa A, Sano T, Negishi A, Yokoo S, Oyama T. Immunohistochemical staining patterns of cytokeratins 13, 14, and 17 in oral epithelial dysplasia including orthokeratotic dysplasia. Pathol Int 2014;64(1):20–7.
[23] Shulman HM, Cardona DM, Greenson JK, et al. NIH Consensus development project on criteria for clinical trials in chronic graft-versus-host disease: II. The 2014 Pathology Working Group Report. Biol Blood Marrow Transplant 2015;21(4):589–603.
[24] Acosta-Rodriguez EV, Rivino L, Geginat J, et al. Surface phenotype and antigenic specificity of human interleukin 17-producing T helper memory cells. Nat Immunol 2007;8(6):639–46.
[25] Levine JE, Braun TM, Harris AC, et al. A prognostic score for acute graft-versus-host disease based on biomarkers: a multicentre study. Lancet Haematol 2015;2(1): e21–9.
[26] Paczesny S, Hakim FT, Pidala J, et al. National Institutes of Health Consensus Development Project on Criteria for Clinical Trials in Chronic Graft-versus-Host Disease: III. The 2014 Biomarker Working Group Report. Biol Blood Marrow Transplant 2015;21(5):780–92.
[27] Arend WP, Palmer G, Gabay C. IL-1, IL-18, and IL-33 families of cytokines. Immunol Rev 2008;223:20–38.
[28] Vignali DA, Kuchroo VK. IL-12 family cytokines: immunological playmakers. Nat Immunol 2012;13(8):722–8.
[29] Joseph RW, Bayraktar UD, Kim TK, et al. Vitamin D receptor upregulation in alloreactive human T cells. Hum Immunol 2012;73(7):693–8.
[30] Lin CC, Bradstreet TR, Schwarzkopf EA, et al. Bhlhe40 controls cytokine production by T cells and is essential for pathogenicity in autoimmune neuroinflammation. Nat Commun 2014;5:3551.
[31] von Essen MR, Kongsbak M, Schjerling P, Olgaard K, Odum N, Geisler C. Vitamin D controls T cell antigen receptor signaling and activation of human T cells. Nat Immunol 2010;11(4):344–9.
[32] Kang BH, Shim YJ, Tae YK, et al. Clusterin stimulates the chemotactic migration of macrophages through a pertussis toxin sensitive G-protein-coupled receptor and Gbetagamma-dependent pathways. Biochem Biophys Res Commun 2014;445(3): 645–50.
[33] Shim YJ, Kang BH, Jeon HS, et al. Clusterin induces matrix metalloproteinase-9 expression via ERK1/2 and PI3K/Akt/NF-kappaB pathways in monocytes/macrophages. J Leukoc Biol 2011;90(4):761–9.
[34] McMahon SB, Van Buskirk HA, Dugan KA, Copeland TD, Cole MD. The novel ATM-related protein TRRAP is an essential cofactor for the c-Myc and E2F oncoproteins. Cell 1998;94(3):363–74.

[35] Porstmann T, Santos CR, Griffiths B, et al. SREBP activity is regulated by mTORC1 and contributes to Akt-dependent cell growth. Cell Metab 2008;8(3):224–36.

[36] Zhang S, Sun G, Wang Z, Wan Y, Guo J, Shi L. PCAF-mediated Akt1 acetylation enhances the proliferation of human glioblastoma cells. Tumour Biol 2015;36(3): 1455–62.

[37] Chinnadurai G. The transcriptional corepressor CtBP: a foe of multiple tumor suppressors. Cancer Res 2009;69(3):731–4.

[38] Wei S, Wang L, Zhang L, et al. ZNF143 enhances metastasis of gastric cancer by promoting the process of EMT through PI3K/AKT signaling pathway. Tumour Biol 2016; 37(9):12813–21.

[39] Borthwick LA, Parker SM, Brougham KA, et al. Epithelial to mesenchymal transition (EMT) and airway remodelling after human lung transplantation. Thorax 2009;64 (9):770–7.

[40] Nikitorowicz-Buniak J, Denton CP, Abraham D, Stratton R. Partially Evoked Epithelial-Mesenchymal transition (EMT) is Associated with increased TGFbeta Signaling within Lesional Scleroderma Skin. PLoS One 2015;10(7):e0134092.

[41] Ding X, Yang DR, Xia L, et al. Targeting TR4 nuclear receptor suppresses prostate cancer invasion via reduction of infiltrating macrophages with alteration of the TIMP-1/ MMP2/MMP9 signals. Mol Cancer 2015;14:16.

[42] Kumawat K, Menzen MH, Slegtenhorst RM, Halayko AJ, Schmidt M, Gosens R. TGF-beta-activated kinase 1 (TAK1) signaling regulates TGF-beta-induced WNT-5A expression in airway smooth muscle cells via Sp1 and beta-catenin. PLoS One 2014;9 (4):e94801.

[43] Liang X, Zeng J, Wang L, et al. Histone demethylase RBP2 promotes malignant progression of gastric cancer through TGF-beta1. (p-Smad3)-RBP2-E-cadherin-Smad3 feedback circuit Oncotarget 2015;6(19):17661–74.

[44] Qiu X, Zhu J, Sun Y, et al. TR4 nuclear receptor increases prostate cancer invasion via decreasing the miR-373-3p expression to alter TGFbetaR2/p-Smad3 signals. Oncotarget 2015;6(17):15397–409.

[45] Fontana MF, Baccarella A, Pancholi N, Pufall MA, Herbert DR, Kim CC. JUNB is a key transcriptional modulator of macrophage activation. J Immunol 2015;194(1): 177–86.

[46] Langlais D, Barreiro LB, Gros P. The macrophage IRF8/IRF1 regulome is required for protection against infections and is associated with chronic inflammation. J Exp Med 2016;213(4):585–603.

[47] Jagasia MH, Greinix HT, Arora M, et al. National Institutes of Health Consensus Development Project on Criteria for Clinical Trials in Chronic Graft-versus-Host Disease: I. The 2014 Diagnosis and Staging Working Group report. Biol Blood Marrow Transplant 2015;21(3) [389-401 e1].

[48] Ali N, Flutter B, Sanchez Rodriguez R, et al. Xenogeneic graft-versus-host-disease in NOD-scid IL-2Rgammanull mice display a T-effector memory phenotype. PLoS One 2012;7(8):e44219.

[49] Ito R, Katano I, Kawai K, et al. Highly sensitive model for xenogenic GVHD using severe immunodeficient NOG mice. Transplantation 2009;87(11):1654–8.

[50] King MA, Covassin L, Brehm MA, et al. Human peripheral blood leucocyte non-obese diabetic-severe combined immunodeficiency interleukin-2 receptor gamma chain gene mouse model of xenogeneic graft-versus-host-like disease and the role of host major histocompatibility complex. Clin Exp Immunol 2009;157(1):104–18.

[51] Mutis T, van Rijn RS, Simonetti ER, et al. Human regulatory T cells control xenogeneic graft-versus-host disease induced by autologous T cells in RAG2−/−gammac −/− immunodeficient mice. Clin Cancer Res 2006;12(18):5520–5.

[52] van Rijn RS, Simonetti ER, Hagenbeek A, et al. A new xenograft model for graft-versus-host disease by intravenous transfer of human peripheral blood mononuclear cells in RAG2−/− gammac−/− double-mutant mice. Blood 2003;102(7): 2522–31.

[53] Hyvarinen K, Ritari J, Koskela S, et al. Genetic polymorphism related to monocyte-macrophage function is associated with graft-versus-host disease. Sci Rep 2017;7 (1):15666.

[54] Delaney TA, Morehouse C, Brohawn PZ, et al. Type I IFNs Regulate Inflammation, Vasculopathy, and Fibrosis in Chronic Cutaneous Graft-versus-Host Disease. J Immunol 2016;197(1):42–50.

[55] Veldhoen M, Hocking RJ, Atkins CJ, Locksley RM, Stockinger B. TGFbeta in the context of an inflammatory cytokine milieu supports de novo differentiation of IL-17-producing T cells. Immunity 2006;24(2):179–89.

[56] Chomarat P, Banchereau J, Davoust J, Palucka AK. IL-6 switches the differentiation of monocytes from dendritic cells to macrophages. Nat Immunol 2000;1(6):510–4.

[57] Kroger N, Solano C, Wolschke C, et al. Antilymphocyte Globulin for Prevention of Chronic Graft-versus-Host Disease. N Engl J Med 2016;374(1):43–53.

[58] Soiffer RJ, Kim HT, McGuirk J, et al. Prospective, Randomized, Double-blind, phase III Clinical Trial of Anti-T-Lymphocyte Globulin to Assess Impact on Chronic Graft-Versus-Host Disease-Free Survival in patients Undergoing HLA-Matched Unrelated Myeloablative Haematopoietic Cell Transplantation. J Clin Oncol 2017;35(36): 4003–11.

[59] Cutler CS, Koreth J, Ritz J. Mechanistic approaches for the prevention and treatment of chronic GVHD. Blood 2017;129(1):22–9.

[60] Koreth J, Kim HT, Jones KT, et al. Efficacy, durability, and response predictors of low-dose interleukin-2 therapy for chronic graft-versus-host disease. Blood 2016;128 (1):130–7.

[61] Koreth J, Matsuoka K, Kim HT, et al. Interleukin-2 and regulatory T cells in graft-versus-host disease. N Engl J Med 2011;365(22):2055–66.